

# Polyelectrolyte-Aided Synthesis of Gold and Platinum Nanoparticles: Implications in Electrocatalysis and Sensing

Chepuri R. K. Rao\*

Functional Materials Division, Central Electrochemical Research Institute, Karaikudi 630006, India

Received 4 May 2011; accepted 25 August 2011

DOI 10.1002/app.35534

Published online 6 December 2011 in Wiley Online Library (wileyonlinelibrary.com).

**ABSTRACT:** An electrochemical method for depositing redispersible, lower size gold nanoparticles from a novel polyelectrolyte-gold complex is described. The size of gold nanoparticles is in the range 6.2–15.4 nm. The gold nanoparticles, first deposited on platinum surface are transferable into water. They can also be directly *in situ*-electrodeposited on to materials like carbon, carbon nanotubes or conducting polymers for an end use as electro catalysts. The composites

Au-MWCNT, Pt-MWCNT, Au-Carbon, and Pt-Carbon are synthesized and tested for their electrocatalytic activity. The composites exhibit good catalytic activity in sensing dopamine or electrooxidation of methanol. © 2011 Wiley Periodicals, Inc. *J Appl Polym Sci* 124: 4765–4771, 2012

**Key words:** polyelectrolyte; gold; platinum; methanol; oxidation catalyst

## INTRODUCTION

Metal nanoparticles exhibit size-dependent properties which are different from their bulk properties,<sup>1</sup> because of which they are useful for varied applications, such as in catalysis and biology.<sup>2–5</sup> Noble metallic particles of Pt, Pd, Ru, and Au are very useful materials in the area of electrocatalysis<sup>6,7</sup> and their chemical or electrochemical deposition methods are prime important for fabrication of catalytically active electrodes.<sup>6</sup> Gold nanoparticles are class of materials which are used in biosensors, substrates for surface enhanced Raman scattering (SERS), catalysis, information storage, nanophotonics, and nanomedicine.<sup>8–12</sup> Gold nanoparticles are useful material for sensing some biologically active molecules such as dopamine in the presence of ascorbic acid, uric acid, and others.<sup>13,14</sup> Primarily gold nanoparticles efficiently tunnel electrons between the electrode and the electrolyte and help in enhancing the signal.<sup>15</sup> Apart from this, gold electrooxidizes many organic molecules<sup>16</sup> including methanol in appropriate pH conditions.<sup>17</sup>

Platinum nanoparticles are inevitably used noble metal in low temperature fuel cells for their excellent electrocatalytic activity. One of the most advanced low temperature fuel cells is the direct methanol fuel cell (DMFC). The challenging issues in DMFC technology are methanol crossover, slow kinetics of

methanol oxidation due to carbon monoxide poisoning effects. The platinum metal is usually dispersed on carbon supports by chemical reduction of platinum salts; electrochemical reduction is seldom used. The contemporary research is focused on the construction of more active anode electrocatalyst materials which would provide higher efficiencies in methanol oxidation and to electrooxidize adsorbed CO to CO<sub>2</sub> efficiently. The best way to negotiate with problem is to design platinum based bimetallic Pt-M type catalysts.<sup>18</sup> Many chemical methods such as coimpregnation, coprecipitation, absorption of colloids<sup>19</sup> are known in literature, the electrochemical reduction methods are limited, though this method is known to give particles with controlled size.<sup>20–22</sup> Recently, carbon nanotubes (CNTs) have been reported to be superior supporting materials compared with carbon black for methanol electro-oxidation.<sup>23,24</sup> CNTs and conducting polymer composite materials provide three-dimensional distributions of Pt particles, leading to enhancement in catalytic activity from the increased electrochemical active surface area (ESA), enhanced charge transfer rate, and electronic conductivity.<sup>25–27</sup>

Here we describe an easy electrochemical method to deposit lower size gold nanoparticles on to the platinum/or stainless steel/or ITO electrodes which can be later transferable to water by simple sonication. The method is aided by the presence of polyelectrolyte, namely, polydiallyldimethylammonium-chloride (PDDMAC) which is present in excess concentrations. The polyelectrolyte PDDMAC serves as not only supporting electrolyte for the electrochemical deposition but also, a source for gold in the form of a complex.

*Present address:* Organic coatings and Polymers Division, Indian Institute of Chemical Technology, Hyderabad-500 007, India..

*Correspondence to:* C. R. K. Rao (rkkousik@rediffmail.com).

The method is also useful to deposit platinum (or gold) nanoparticles directly on to the materials like carbon, polypyrrole, and carbon nanotubes. We present our results on deposition of gold and platinum particles on to the carbon (Black Pearl), polypyrrole, and MWCNTs and some of their catalytic activity in methanol oxidation and dopamine sensing reactions.

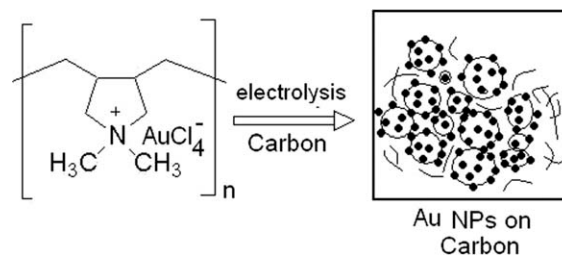
## EXPERIMENTAL

MWCNTs (110–170 nm diameter, 5–9  $\mu\text{M}$  in length), PDDMAC (35 wt % in water,  $M_w \sim 100,000$ ) were purchased from Aldrich Chemical Company. The analytically pure  $\text{AuCl}_3$  and  $\text{K}_2\text{PtCl}_6$  were purchased from Arora Matthey, India. XPS analysis of the sample was done using the Multilab 2000 (Thermoscientific, UK) photoelectron spectrometer fitted with a twin anode x-ray source. The  $4f$  core-level photoemission spectra for Au and Pt were recorded using the  $\text{MgK}_{\alpha}$  (1253.6 eV) source. XRD measurements were carried out on a Philips Pananalytical X-ray diffractometer using Cu K $\alpha$  radiation ( $k = 0.15406$  nm). The identification of the phases was made by referring to the Joint Committee on Powder diffraction Standards International Center for Diffraction Data (JCPDS-ICDD) database. To estimate the particle size Scherrer's equation was used. For this purpose, the (111) peak of Au or Pt (in fcc structure) which appears around  $2\theta = 38\text{--}40$  was selected. SEM measurements were made using Hitachi SEM, model-3000H instrument. The EDAX measurements for estimation of metal loading were taken on THERMO (electron corporation) SUPER DRY-II connected to XRD facility. Electrochemical deposition was performed on AUTOLAB 302 electrochemical system. TEM experiments were conducted on FEI make Tecnai-20-G<sup>2</sup> machine with tungsten filament at 200 kV.

### Synthesis of gold nanoparticles

In a typical synthesis, 20 mg of  $\text{AuCl}_3$  ( $6.6 \times 10^{-5}$  M) in 10 mL of water is mixed into 10 mL of 40% aqueous solution of PDDMAC, further diluted by 20 mL of water and ultrasonicated for 15 min. Gold nanoparticles were deposited onto either sides Pt foil (8 mm  $\times$  10 mm) cathode by applying a current density of 1 mA  $\text{cm}^{-2}$  on the Pt foil anode (10 mm  $\times$  10 mm) for 15 min. After the end of the electrolysis, the deposited gold nanoparticles were transferred into water (10 mL) by sonication of the gold-deposited electrode and the resultant gold sol is used for SPR and TEM investigations.

Dopamine sensing and methanol oxidation were investigated by a GC electrode-modified by loading 5  $\mu\text{L}$  of electrocatalyst ink. The ink was prepared by mixing 2.5 mg of metal composite, 200  $\mu\text{L}$  of 5%



**Scheme 1** Scheme showing novel gold complex undergoing electroreduction to form dispersible gold nanoparticles on platinum surface with trapped polymer.

Nafion solution, and 800  $\mu\text{L}$  of water. The mix was sufficiently sonicated to give a uniform dispersion. From this 5  $\mu\text{L}$  of the catalyst was loaded on to the GC electrode and dried at R.T. The electrochemical sensing of dopamine and methanol oxidation were performed using phosphate buffer (pH 7.0) and in 0.5 M sulfuric acid, respectively.

## RESULTS AND DISCUSSION

As described in our earlier article,<sup>28</sup>  $\text{AuCl}_3$  forms an anionic complex,  $\text{AuCl}_4^-$  in chloride rich PDDMAC aqueous solution and acts as source for the gold nanoparticles (Scheme 1). As we understand, the role of PDDMAC is trifunctional. First, it acts as counter anion for the  $\text{AuCl}_4^-$  complex species. PDDMAC<sup>+</sup> is a big macro-molecule compared with small  $\text{AuCl}_4^-$ . Hence diffusion of PDDMAC<sup>+</sup> is difficult and it is believed that only  $\text{AuCl}_4^-$  species moves along the positively charged back-bone of PDDMAC. Thus big cation- small anion electrostatic interactions result in regulated diffusion of  $\text{Au}^{3+}$  towards cathode and help in formation of lower size gold particles. Second, PDDMAC acts as self supporting electrolyte for the electrolytic cell and reduces cell voltage. Third, PDDMAC is codeposited along with gold nanoparticles and help in redispersability into water.

The water redispersed gold nanoparticles with pale brownish pink color, exhibited a surface plasmon band at 544nm in water (Fig. 1) and are in dispersed phase up to 24 h in pure water. The stability of the dispersion can be extended to few days by the addition of few drops 1% PDDMAC solution. Formation of the gold nanoparticles is also evident from X-ray diffraction profile of the particles, deposited onto carbon or MWCNTs (Fig. 1). The profile for Au/C showed (111), (200), (220), (311), and (222) planes of f.c.c gold at  $2\theta = 38.41, 44.56, 64.77, 77.72, 81.80$ .

The redispersibility of the deposited gold nanoparticles from platinum electrode into water is facilitated by the codeposition of PDDMAC polymer. The presence of water soluble PDDMAC in the electrodeposit makes the gold nanoparticles bound loosely to

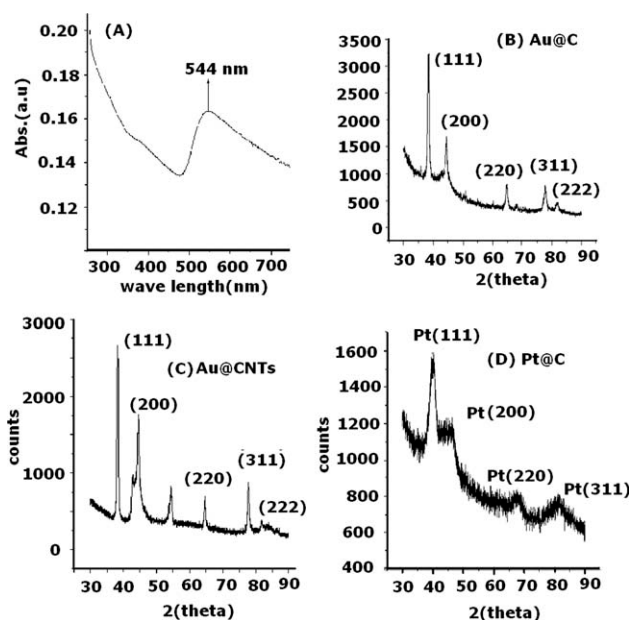


**Figure 1** (a) SPR band of gold nanoparticles deposited on Pt electrode which are redispersed in water. (b) XRD profile of Au particle on blackpearl carbon. (c) XRD profile of Au-MWCNTs and (d) XRD profile of Pt-Carbon composite.

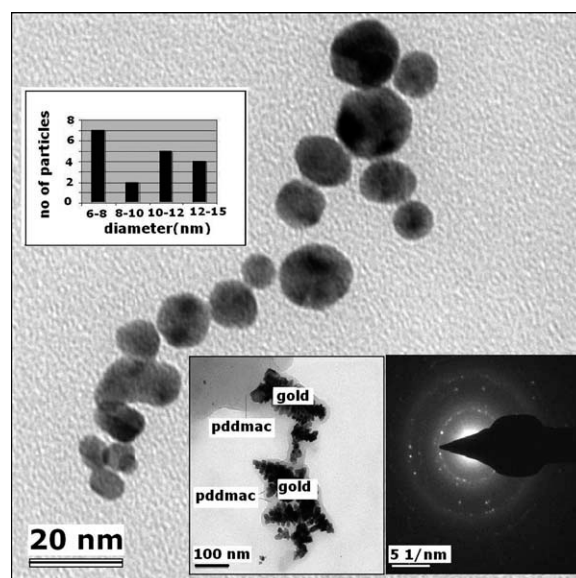
the base platinum electrode. The presence of polymer in the deposit is evident from TEM and XPS analyses of the samples. After thorough washing and sonication of the samples, individual particles are seen (Fig. 2) whose sizes are in the range 6–15 nm. The particles are seen as round or oval type platelets without bound polymer. In unwashed samples, one can clearly distinct gold nanoparticles encapsulated in polymer matrix (Fig. 2, inset). These particles lose protecting PDDMAC layers after repeated washings with water. The presence of PDDMAC in the deposit is also evidenced by appearance of a peak at 401.5 eV due to tetravalent  $=N^+=$  species arising from PDDMAC in the XPS spectrum.<sup>29</sup> Figure 3(a) shows survey spectrum of the gold nanoparticles deposited on platinum foil. Figure 3(c) shows peak due to  $=N^+=$  species. The spectrum also showed a couplet due to Au(0) species at 87.5 and 83.8 eV originating from 4f shell of Au(0) atoms [Fig. 3(b)]. These values are comparable to literature values for gold in zero valence state.<sup>30</sup>

The utility of the gold nanoparticles is demonstrated in the electrocatalytic oxidation (sensing) of dopamine. Dopamine (DA) is an important neurotransmitter and the loss of DA-containing neurons may lead to serious disease known as Parkinson's disease. The electrochemical detection of DA has therefore been a subject of considerable interest in recent times in electroanalytical chemistry. DA is electrochemically oxidized to the corresponding quinone on modified GC surface to dopamine-*o*-qui-

none form. Following the initial oxidation, 1,4-addition reaction can occur, forming a cyclized product called a leucochrome. At low pH values, the open-chain quinones are protonated to a great extent, and the cyclization reaction is unfavorable. At higher pH values, a sufficient amount of unprotonated quinone is available so that cyclization is observed. The leucochrome formed in the vicinity of the electrode following the 2-electron oxidation can be observed as a reductive wave at potentials negative of that for the reduction of the noncyclized quinone.

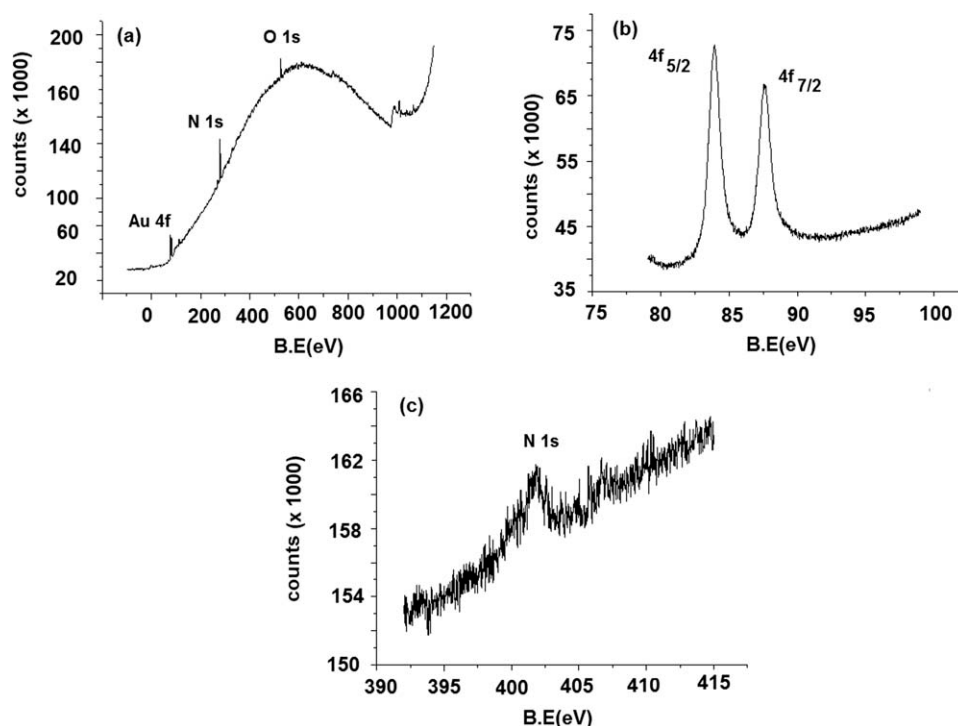
For this purpose, gold nanoparticles were directly deposited on multiwalled carbon nanotubes (MWCNT) by introducing the CNTs in the electrolytic cell during electrosynthesis. Figure 4, inset shows gold nanoparticles (1.78 wt %) deposited MWCNTs (Au-CNT). The XRD profile is shown in Figure 1(c). The expected (111), (200), (220), (311) and (222) reflections observed at  $2\theta = 38.28, 44.43, 64.65, 77.64,$  and  $81.83,$  respectively. The peak at  $2\theta = 54.27$  is due to MWCNTs. The gold nanoparticle size estimated from (111) peak is 18.4 nm.

Figure 4 shows CV of electrochemical oxidation of DA performed by Au-CNTs/GC electrode ( $C_{\text{dopa}} = 0.5 \times 10^{-5} M$ ). In presence of catalyst Au-CNT (0.3 mg on  $0.0314 \text{ cm}^2$  GC electrode), the current density corresponding to DA oxidation at 0.232 V increased to  $3.05 \mu\text{A cm}^{-2}$  compared to  $1 \mu\text{A cm}^{-2}$  with pure GC electrode. It is observed that the current density of the oxidation peak increased with the



**Figure 2** TEM pictures of gold nanoparticles deposited on Pt electrode which are redispersed in water with size distribution and SAED pattern in the inset. Another inset is TEM picture of gold nanoparticles which are redispersed in water before washing showing the presence of PDDMAC polymer.





**Figure 3** XPS spectrum of gold nanoparticles deposited on Pt foil (a) survey spectrum (b) zoomed spectrum showing the presence of Au(0) (c) zoomed spectrum showing the presence of  $=N^+$  species from PDDMAC.

$C_{\text{dopa}}$  (10–250  $\mu\text{M}$ ) (Fig. 4). The peak current density showed a linear relationship with  $C_{\text{dopa}}$  (inset, Fig. 4).

In this case, it is to be noted that though oxidation peak current (and reduction peak current) is increased with the gradual addition of DA, there is a slight positive shift in the potentials. This is because there is only a low level of loading of the composite is possible by the adsorption process which leads to

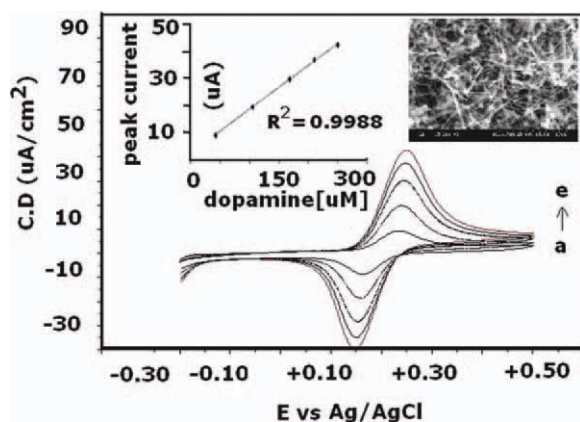


**Figure 4** CV profiles of dopamine oxidation exhibited by Au-MWCNT/GC electrode in phosphate buffer pH 7.0 at a scan rate of  $50 \text{ mV s}^{-1}$ . Concentrations of dopamine (a)  $42 \mu\text{M}$  (b)  $104 \mu\text{M}$  (c)  $168 \mu\text{M}$  (d)  $210 \mu\text{M}$  (e)  $250 \mu\text{M}$ . Inset shows the linear relation between peak current and  $C_{\text{dopa}}$ . Other inset shows the morphology of the composite as shown by SEM. [Color figure can be viewed in the online issue, which is available at [wileyonlinelibrary.com](http://wileyonlinelibrary.com).]

ratio-mismatch between the concentration of the composite and dopamine at higher concentrations of DA.<sup>28</sup> Fouling of the modified electrode due to the adsorption of polymeric product<sup>31</sup> may also be another reason. Thus gold nanoparticles deposited CNTs are useful in sensing dopamine in concentration as low as  $5 \mu\text{M}$ .

The polyelectrolyte process is adopted to deposit platinum nanoparticles on Pt foil or directly on MWCNTs similar to gold nanoparticles. A platinum loading of 5.01 wt % on MWCNTs was confirmed by EDAX method. Figure 5 shows scanning electron micrographs of Pt nanoparticles deposited on platinum foil for 0.5 h using a current density of  $1 \text{ mA cm}^{-2}$ . The deposit is thick and clusters of Pt nanoparticles in the range 50–200 nm are seen as globules. The XPS spectrum of this sample exhibited a doublet type spectrum at 71.5 and 74.8 eV ( $4f_{7/2}$  and  $4f_{5/2}$ ) suggesting platinum in zero valence.<sup>32</sup> The XRD profile of the Pt-MWCNTs exhibited peaks due to (111), (200), (220), (311) at  $2\theta = 39.90, 46.60, 68.10, \text{ and } 81.70$ , respectively. The average particle size deduced from this data is 5.65 nm. The XRD profile for the Pt-C is shown in Figure 1(d) which showed the above reflections at  $2\theta = 40.01, 46.51, 68.31, \text{ and } 81.67$  with estimated particle size as 5.57 nm. As revealed by TEM studies on Pt-MWCNTs, the platinum particles are deposited on MWCNTs (Fig. 6) with different cluster sizes in the range 5–50 nm. The Pt-MWCNTs composite is shown to be good electrocatalyst for oxidation of methanol.

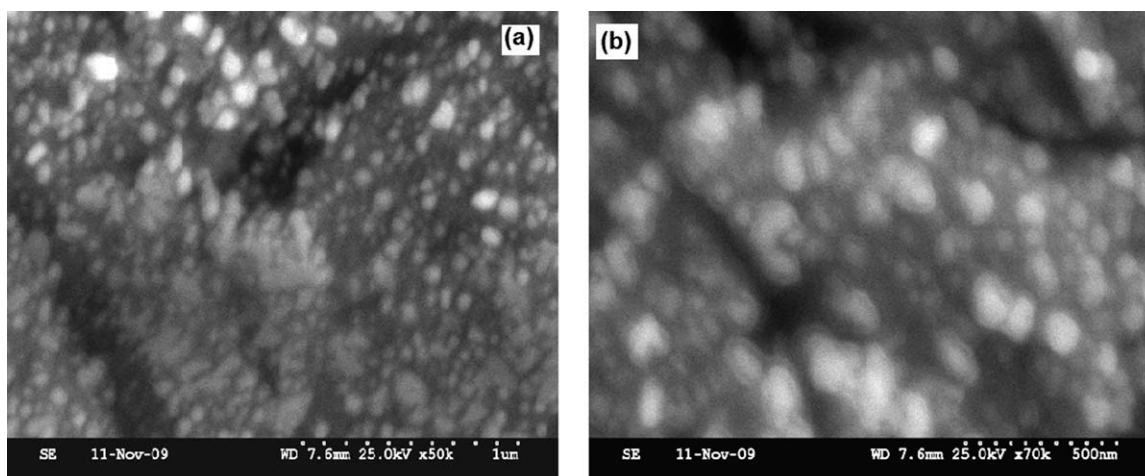


**Figure 5** SEM pictures of Pt nanoparticles deposited on Pt foil shown at (a)  $\times 50,000$  (b)  $\times 70,000$  magnifications.

In absence of BET surface area analyzer, we estimated the specific surface area ( $S$ ) of Pt particles on MWCNTs from the relation<sup>33</sup> (from XRD data).

$$S = 6000/\rho \times d$$

where  $\rho$  and  $d$  are density and mean crystallite size of Pt particles.

Table I lists the physical properties of the synthesized composites. The surface area for gold nanoparticles is in the range  $11\text{--}17\text{ m}^2\text{ g}^{-1}$  with size of the gold particles in the range  $18\text{--}28\text{ nm}$ . The smaller platinum particles on carbon or MWCNTs (i.e.,  $5\text{--}6\text{ nm}$ ) showed higher surface area of the composite around  $50\text{ m}^2\text{ g}^{-1}$ . The electrochemical active surface area (EAS) calculated from hydrogen adsorption/desorption curves in

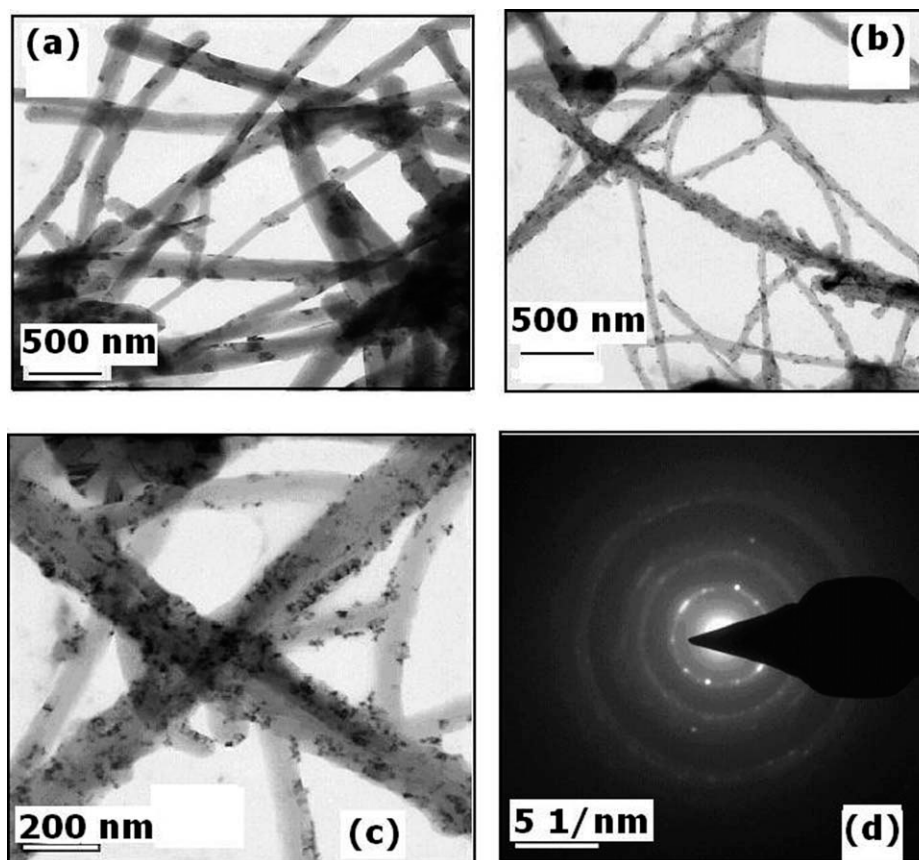


**Figure 6** TEM pictures (a,b,c) of Pt nanoparticles on MWCNTs and (d) SAED picture of the composite.

**TABLE I**  
**Properties of the Gold and Platinum Nanocomposites**

Composite	Metal loading (wt %) <sup>a</sup>	Metal particle size <sup>b</sup> (nm)	Surface area (m <sup>2</sup> g <sup>-1</sup> ) XRD <sup>b</sup> (EAS) <sup>c</sup>	Potential and C.D for MOR V[(uA cm <sup>-2</sup> )]	Potential and C.D for dopamine ox. V[(uA cm <sup>-2</sup> )]
Au-CNT	1.80	18.4	16.89	na	0.232 (3)
Au-PPY	1.78	26.0	11.90	na	na
Au-C(bp)	1.65	28.15	11.04	na	0.390 (24)
Pt-CNT	5.01	5.65	50.00 (47.1)	0.73 (28)	0.219 (2.7)
Pt-C(bp)	<1.0	5.57	50.33 (47.6)	na	0.217 (1.3)

Potentials are with reference to Ag/AgCl.

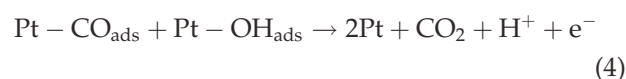
<sup>a</sup> Based on EDAX measurements.

<sup>b</sup> Based on XRD data.

<sup>c</sup> Electrochemically active surface area, based on CV data, na, not active; naa, not appreciably active.

cyclic voltammogram of the Pt-composites also gave similar results (Table I).

The Pt-MWCNT catalyst (0.4 mg on 0.0314 cm<sup>2</sup> GC electrode) showed methanol oxidation peak at 0.730 V (vs. Ag/AgCl) (current density observed =  $0.28 \times 10^{-4}$  A cm<sup>-2</sup>) for 0.5 M MeOH in 0.5 M sulfuric acid solution in the forward scan and another oxidation peak at 0.575 V in the reverse scan (Fig. 7). The bare GC electrode did not show any methanol oxidation peak in this potential region. As shown in Figure 7, during the positive voltage scan, methanol is oxidized to CO and CO<sub>2</sub>, and the surface of the Pt is gradually covered by hydroxide from adsorptive dissociation of water over the potential 0.73 V. Around 0.9 V the surface is fully covered by hydroxide from water decomposition. The negative voltage scan reduces the hydroxide covering the surface, then the adsorbed methanol and reaction intermediates are reoxidized again giving another oxidation peak in the reverse scan, as shown in eqs. (1)–(4) below.



The catalytic efficiency of the MOR is increased to 2.5 times when 1 : 1 mixture of Pt-MWCNT+Au-MWCNT (0.4 mg on 0.0314 cm<sup>2</sup> GC electrode) is used. The current density increased to  $0.73 \times 10^{-4}$  from  $0.28 \times 10^{-4}$  A cm<sup>-2</sup> with a slight decrease of 30 mV in the oxidation potential. This shows that the binary composite is more catalytically active than pure Pt-CNT composite.

In summary, we have demonstrated an efficient method to deposit redispersible gold nanoparticles using polyelectrolyte PDDMAC. The method also allows to deposit electrocatalytically active gold and platinum nanoparticles on materials like carbon, conducting polymers, and carbon nanotubes. It is also demonstrated that composites Au-CNTs and Pt-CNTs are useful in sensing dopamine and electrocatalyze MOR. The method also paves way to deposit palladium and other precious metals for catalytic applications. Significantly, in this preliminary investigation, we also observed that composites Pt-MWCNT, Pt-C, and Au-C are active in sensing dopamine (Table I) and attracted further investigations which will be communicated as full length article.

The author sincerely thanks the Directors ICT and CECRI for their constant encouragement, unstinted support.

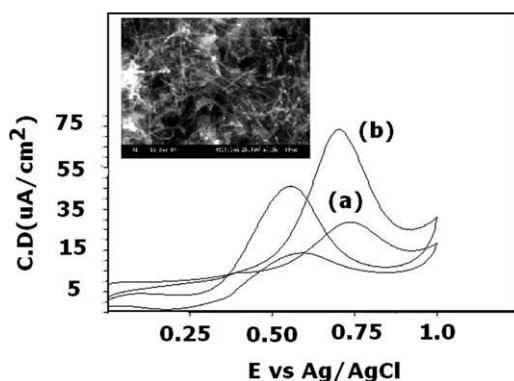


**Figure 7** CV profile of methanol oxidation shown by (a) Pt-MWCNT and (b) Pt-MWCNT + Au-MWCNT electrocatalysts in 0.5M sulfuric acid containing 0.5M methanol at 50 mV s<sup>-1</sup>. Inset shows the morphology of the composite as shown by SEM.

## References

- Rao, C. N. R.; Kulkarni, G. U.; Thomas, P. J.; Edward, P. P. *Chem Soc Rev* 2002, 29, 27.
- Daniel, M. C.; Astruc, D. *Chem Rev* 2004, 104, 293.
- Schmid, G.; Chi, L. F. *Adv Mater* 1998, 10, 515.
- Banerjee, I. A.; Yu, L. T.; Matsui, H. *Nano Lett* 2003, 3, 283.
- Brust, M.; Kiely, C. J. *Colloids Surf A* 2002, 202, 175.
- Rao, C. R. K.; Trivedi, D. C. *Coord Chem Rev* 2005, 249, 613.

7. Tian, N.; Zhou, Z.-Y.; Sun, S.-G. *J Phys Chem C* 2008, 112, 19801.
8. Eustis, S.; El-Sayed, M. A. *Chem Soc Rev* 2006, 35, 209.
9. Murphy, C. J.; Sau, T. K.; Gole, A. M.; Orendorff, C. J.; Gao, J.; Gou, L.; Hunyadi, S. E.; Li, T. *J Phys Chem B* 2005, 109, 13857.
10. Khanal, B. P.; Zubarev, E. R. *Angew Chem Int Ed* 2007, 46, 2195.
11. Stewart, M. E.; Anderton, C. R.; Thompson, L. B.; Maria, J.; Gray, S. K.; Rogers, J. A.; Nuzzo, R. G. *Chem Rev* 2008, 108, 494.
12. Jain, P. K.; Huang, X.; El-Sayed, I. H.; El-Sayed, M. A. *Acc Chem Res* 2008, 41, 1578.
13. Gao, Z.; Huang, H. *Chem Commun* 1998, 2107.
14. Mathiyarasu, J.; Kumar, S. S.; Phani, K. L. N.; Yegnarman, V. *Mater Lett* 2008, 62, 571.
15. Brown, K. R.; Fox, A. P.; Natan, M. J. *J Am Chem Soc* 1996, 118, 1154.
16. Burke, L. D.; Nugent, P. F. *Gold Bull* 1998, 31, 39.
17. Santhosh, P.; Gopalan, A.; Lee, K. P. *J Catalysis* 2006, 238, 177.
18. Peng, Z.; Yang, H. *Nanotoday* 2009, 4, 143.
19. Liu, Z.; Ling, X. Y.; Guo, B.; Hong, L.; Lee, J. Y. *J Power Sources* 2007, 167, 272.
20. Taylor, E. J.; Anderson, E. B.; Vilambi, N. R. K. *J Electrochem Soc* 1992, 139, L45.
21. Verbrugge, M. W. *J Electrochem Soc* 1994, 141, 46.
22. Thompson, S. D.; Jordan, L. R.; Forsyth, M. *Electrochim Acta* 2001, 46, 1657.
23. Carmo, M.; Paganini, V. A.; Rosolen, J. M.; Gonzalez, E. R. *J Power Sources* 2005, 142, 169.
24. Wu, G.; Xu, B.-Q. *J Power Sources* 2007, 174, 148.
25. Zhao, H.; Yang, J.; Zhang, Y. *J Power Sources* 2008, 184, 375.
26. Selvaraj, V.; Alagar, M. *Electrochem Commun* 2007, 9, 1145.
27. Wang, S.; Jiang, S. P.; White, T. J.; Guo, J.; Wang, X. *J Phys Chem C* 2009, 113, 18935.
28. Prakash, S.; Rao, C. R. K.; Vijayan, M. *Electrochim Acta* 2009, 54, 5919.
29. Kuzmany, H. *Solid State Spectroscopy*; Springer-Verlag: Germany, 1998; p 284.
30. Briggs, D.; Seah, M. P. *Practical Surface Analysis*, 2nd ed., Vol.1; Wiley: Chichester, 1990.
31. Xiang, Q.; Lin, L. Z. *Anal Lett* 2001, 34, 1585 and references therein.
32. Morikawa, T.; Ohwaki, T.; Suzuki, K. I.; Moribe, S.; Tero-Kubota, S. *Appl Catal B* 2008, 83, 56.
33. Pozio, A.; De Francesco, M.; Cemmi, A.; Cardellini, F.; Giorgi, L. *J Power Sources* 2002, 105, 13.